International Research Journal of Engineering and Technology (IRJET) e-ISSN: 2395-0056
Volume: 11 Issue: 04 | Apr 2024 www.irjet.net p-ISSN: 2395-0072

PERFORMANCE ANALYSIS OF ELECTRICAL MACHINES USED IN AUTOMOTIVE

Manoj Kumar Bhati[1], Dr. D.K. Bhalla[2]

[1]B.Tech. Mechanical Engineering (Evening) Scholar, School of Mechanical Engineering, Lingaya's Vidyapeeth, Faridabad, Haryana, India
[2]Professor and LEET Coordinator B.Tech., M.Tech., PhD, FIE in Lingaya's Vidyapeeth, Faridabad, Haryana, India

---

Abstract- This essay offers an assessment of the electrical machine needs for automobiles, both in terms of existing and future technology. Initially, 10 distinct electrical machines are compared using market-available electric and hybrid automobiles as the basis. The comparison's objective is to assess the various electrical machine topologies, structures, operational environments, and performance. Several cutting-edge electrical machine design methodologies have been investigated and researched by using them in the 10 machines that are being compared, and the future design needs of electrical machines in automotive are offered. The study's result demonstrates that, among the many electrical machine topologies, permanent magnet topologies perform the best and may be able to accommodate future demands. Additionally, in order to enable electrical devices to run with the necessary power density aim, aggressive cooling techniques like as spray, dripping, semi- or completely flooded, are required. Lastly, it seems that future electrical machines may adopt the design to recycle principle with little to no performance loss.

Key words: Electric vehicle, automobile, and electrical machine electric vehicle

1. INTRODUCTION

Ever since the GM EV1 introduced electrical cars (EVs) to the market in 1996, the automobile industry has acknowledged the potential of this technology to replace internal combustion engines (ICMs). However, the EV1's performance and cost were incomparable to those of the ICM cars because to the infancy of the electrical motor and battery technology at the time. However, because of the worrisome rates of climate change and the ensuing regulations, electrification of transport became a requirement rather than a choice. In order to prevent a drastic shift and to allow for the advancement of battery and motor technologies, the automobile industry has introduced engine electrification and hybrid electrical vehicles (HEVs) as a means of making incremental progress towards clean vehicle technology. Upon examining EV and HEV products from their launch in 1996 until the late 2010s, all of the established topologies—DC field rotor (DC), induction machine (IM), switching reluctance (SR), and permanent magnet (PM)—have been found in automotive applications [1]. As far as the author is aware, SR is the first topology to withdraw from the race; apart from Holden-ECO, SR has not been used in this application. This is due to the fact that the primary difficulties with SR machines are poor power density and torque ripple, both of which are necessary for the automobile industry, as well as the demand for an unusual converter, which raises the drive's overall cost. Additionally, the IM and DC have decreased; at this point, they are only found in Tesla and Renault, respectively. With the majority of electric motors, including those seen in the most recent 2016 Model S from Tesla, the PM has dominated the automobile industry. Automotive applications have used a variety of PM machine topologies, including as internal (IPM), surface-mounted (SPM), and PM-assisted synchronous reluctance (SynRel-PM) [1]. The need for PM material is a significant obstacle even with the widespread use of PM equipment in the automobile industry. Consequently, decreased PM design strategies have been put out and used in the most recent technology. For automotive applications, other permanent magnet types as ferrite and AlNiCo have also been thoroughly investigated [2]. As a result, 10 distinct electrical machine designs that are based on machines found in various EVs and HEVs have been chosen for comparison in this research. The purpose of the research is to assess the various electrical machines' topologies, structures, operating environments, and overall performance. Apart from electromagnetic performance, comparisons have also been made between mechanical and thermal outcomes. Furthermore, by using them in the contrasted machines, many cutting-edge design strategies have been investigated and researched. In order to fulfil future automotive objectives, this research investigates the feasibility of pushing the existing boundaries of electrical machinery.

2. A review of various electrical machine kinds based on market research

Ten cars, including hybrids and fully electric models, are shown in Table 1; their electric motors have been chosen for comparison in this section. The cross section and winding arrangement of the 10 machines are shown in Figure 1. The selection of the machines was based on the availability of their information in the literature [3–15]. The chosen machines feature rotor topologies with DC, IM, and PM, SPM, IPM, and SynRel-PM for PM machines, and one design (based on the Chevrolet Volt 2) with ferrite. The ANSYS package is

used to perform the analyses. Honda Civic (HC) and Accord (HA) models have a focused winding in a traditional SPM arrangement. In the HA, the PMs are mechanically buried in the rotor core frame, whereas in the HC, a retaining sleeve is used. Because segmented stator teeth with focused winding are the designs' merit approaches, automated winding with a high impact factor is advantageous [3]. Nevertheless, in addition to the intricate previously described design elements—buried PM and sleeve—that are necessary for mechanical safety, the SPM structure uses a large amount of PM. One of the most often compared electrical machines is the 2010 Toyota Prius (TP1), which has been the subject of several articles serving as a standard for vehicle design research [4]. This is because the car is successful and the motor's information is publicly accessible. The IPM construction provides a broad power-speed range, high torque per magnet volume, and reluctance torque [5, 6]. Comparably, the IPM rotor construction of the 2014 Toyota Prius (TP2) has a new magnet placed close to the rotor surface. To preserve strong mechanical performance and provide rotor cooling channels, the rotor's mechanical design has complexly formed gaps. The axial length of the two Chevrolet Volt motors (C1) and (C2) is smaller in CV2, despite having separate rotors and the same stator. Both motors are SynRel-PM, with CV2 being one of the few automotive motors having ferrite and CV1 being constructed with a modest amount of NdFeB. Large arc-shape numbers are used in the design to take advantage of ferrite's mass density and inexpensive cost [7-9]. Both the BMW i3 (BI) and the Nissan Leaf (NL) are electric vehicles that are being compared in this research. Both motors have a lower PM amount and a SynRel-PM structure. BI with cutting design methods that emphasise the low magnetic amount advantage of the reluctance torque [10, 11]. NL has an unusual rotor configuration, with smaller magnets arranged in a V shape near the inner radius and larger magnets towards the outside rotor radius [12, 13]. Last but not least are the non-PM Renault Zoe (RZ) and Tesla Model S (TS) machines, which have an IM framework and a conventional DC rotor (field wound, FW) [12, 13]. It's important to note that the RZ rotor is made up of a traditional commutated field winding rotor; all of Renault's HEVs and EVs are DC rotor vehicles [14].

With a sophisticated but creative rotor cooling system, TS IM has addressed the problem of rotor heating [15]. The eight machines' primary design parameters are shown in Table 2. All dispersed windings (DW) and concentrated windings (CW) are assumed to have packing factors of 0.6 and 0.4, respectively. A overview of the 10 machines' electromagnetic load and open circuit findings is shown in Table 3. The torque density in the PM topologies is comparable, almost double that of the non-PM topologies. Similar trends are seen in power density, with PM topologies having values that are three to four times higher than those of non-M topologies. Due to its many low mass density ferrite particles and several flux routes that provide increased reluctance torque, the CV2 ferrite architecture stands out.

The machine's estimated cost is determined by criteria such as torque and power per magnet weight. In addition to SPM topologies, which make the optimal use of PM material, SynRel topologies outperform IPM in terms of torque and power per magnet weight. Furthermore, because of their large number of turns and low voltage input, HA and HC are shown to be the best when using the inverter kVA, which measures torque per kVA and power per kVA. On the other hand, SynRel topologies have the maximum power per current density when compared to non-PM topologies, when considering the utilisation of current density. There is also more torque per current density in the SynRel topologies. This demonstrates how the SynRel uses the reluctance torque more than the IPM.

3. Result Analysis

An overview of the machines under comparison's performance:

• When compared to other PM machines, NL has the greatest power density, the most mild current density, and a temperature rise as a result. However, it falls short in terms of torque density and torque per volume.

• Because CV2 is the sole topology using ferrite magnets, it provides a high power density and power per volume. The ferrite's low mass density results in a modest overall weight. The increased power capacity of CV2 is also attributed to its high current density and the intense cooling that is necessary for it. The TP1 and TP2 are small and hence light-weight machines, but the speed capability is mechanically limited by high stress resulting from the rotor shape. High power and torque density as well as high power and torque per volume are the results of this. These devices are susceptible to rapid temperature increase, nevertheless, because of their compact size and high power density. Because of the tiny rotor diameter, which has a positive effect on mechanical performance and reduces stress, greater speed operation is possible.

• The maximum power density, torque density, and torque per volume are found in PM topologies with IPM and PMSR rotor configurations. With rigorous cooling techniques, the performances' moderate to high current density allows for a controlled temperature increase. Furthermore, these topologies offer high power and torque utilisation per current density, meaning they make effective use of the current density. Unfortunately, the high mechanical stress caused by the rotor design in certain PM machines restricts the speed range.

Table 1 lists the electric motors for the study's hybrid and electric cars.

Vehicle	Year	Type	Acronym
Honda Accord	2005	Hybrid	HA
Honda Civic	2005	Hybrid	HC
Toyota Prius	2010	Hybrid	TP1
Toyota Prius	2018	Hybrid	TP2
Chevrolet Volt	2016	Hybrid	CV1
Chevrolet Volt	2016	Hybrid	CV2
BMW i3	2014	Full electric	BI
Nissan Leaf	2012	Full electric	NL
Renault Zoe	2014	Hybrid	RZ
Tesla Model S	2012	Full electric	TS

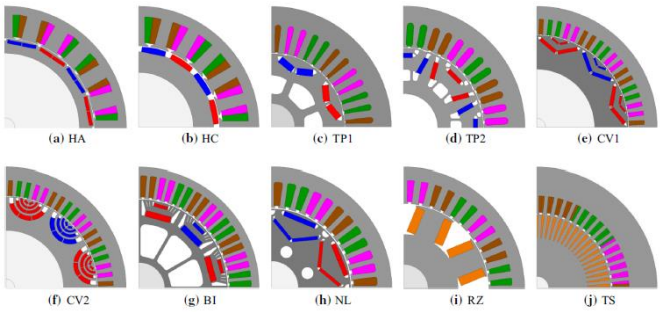

Figure 1: Cross sections of the machines under study. (a) HC (b) HA (c) CV1 (f) CV2 (g) TP1 (d) TP2 (e) NL (i), RZ (j), TS, BI (h),

Table 2: Study Machine Design Parameters and Specifications

Specifications	HA	HC	TP1	TP2	CV1	CV2	BI	NL	RZ	TS
Topology	SPM	SPM	IPM	IPM	IPM	PMSR	PMSR	IPM	FW	IM
Winding type	C-DL	C-DL	D-SL	D-SL	D-SL	D-SL	D-SL	D-SL	D-SL	D-DL
Coils per phase	8	8	8	8	12	12	12	8	8	12
Turns per coil	52	55	11	4	4	4	6	6	6	1
Parallel paths	8	8	1	1	1	1	3	2	2	2
Peak current density (A/mm^2)	10.9	13.5	43.3	59.9	25.3	25.3	16.8	31.4	26.7	24.24
Peak phase current (A)	225	250	235	700	325	325	400	480	480	900
DC bus voltage (V)	144	144	650	200	360	360	380	360	360	360
Drive kVA	32.4	36	152	140	117	117	141	168	172	324
Stator slots	24	24	48	48	72	72	72	48	48	60
Rotor pole pairs	8	8	8	8	12	12	6	4	8	4
Stator outer diameter (mm)	335	265	264	214	340	340	242	198.12	250	254
Axial length (mm)	40	40	50.8	60	51.5	31.5	132	151.16	155	152
Total active volume (mm^3 E06)	3.53	2.21	2.78	2.16	4.68	2.86	8.56	4.93	7.61	7.7
Permanent magnet weight (kg)	0.79	0.79	1.39	0.66	4.2	0.9	2	1.7	–	–
Armature winding copper weight (kg)	5.5	4.7	0.78	3	1.53	4.1	7.1	4.7	6.09	6.75
Rotor copper weight (kg)	–	–	–	–	–	–	–	–	3.4	6.67
Steel weight (kg)	13.2	8.7	13.9	11.5	21.5	11.9	32.3	24.3	36.4	45.9
Total motor weight (kg)	22.86	18.22	19.08	15.9	30.15	19.6	42	33.1	48.6	60.3

C-DL concentrated double layers, *D-SL* distributed single layer, and *D-DL* distributed double layers

RZ and TS, two magnet-less topologies, are capable of achieving high power and torque densities. However, since these machines use rotors with active copper, rotor temperature is a problem. However, the variable field current of the RZ wrapped field machine provides superior field weakening capabilities, although at the anticipated cost of commutator complexity and losses.

Table 3: Performance overview of the devices under study

Performance	Unit	HA	HC	TP1	TP2	CV1	CV2	BI	NL	RZ	TS
Cogging torque (pk-pk)	Nm	10.97	8.97	1.31	0.53	3.34	0.45	2.6	18.8	16.19	–
Back-EMF fundamental, at rated speed	V	111.3	113.6	146.2	41.6	174.6	34.9	116.7	127.09	185.9	–
Back-EMF THD, at rated speed	–	6.03	9.18	17.45	8.8	14.74	15.11	11.2	9.19	15.94	–
Torque ripple, at peak current	–	18.47	3.51	9.79	31.2	21.65	28.78	25	10.9	27.03	8.99
Average torque, at peak current	Nm	119.5	122.8	227.9	191	309.8	130.1	300	314.7	339	330
Torque per volume	Nm/mm^3E06	33.88	55.57	81.98	88.4	66.20	45.51	35	63.85	44.56	42.8
Torque density	Nm/kg	5.22	6.73	11.9	12	10.27	6.63	6.45	9.5	6.97	5.47
Torque per KVA	Nm/kVAE03	3.69	3.41	1.5	1.36	2.65	1.11	2.12	1.87	1.97	1.01
Torque per magnet weight	Nm/kg	151.2	155.4	163.9	289	73.76	118.2	93.75	185	–	–
Torque per current density	$Nm/A/mm^2$	10.97	9.10	5.26	3.18	12.25	5.15	17.8	10.03	12.70	13.61
Maximum output power	kW	27.2	31	77	68.4	100.4	78.2	121	154	90.2	250
Power per volume	kW/mm^3E06	7.71	14.03	27.69	31.6	21.45	27.34	14	31.24	11.85	32.4
Power density	kW/kg	1.18	1.7	4.03	4.3	3.3	3.9	2.6	4.65	1.85	4.1
Power per KVA	kW/kVA	0.84	0.86	0.5	0.48	0.86	0.67	0.85	0.92	0.52	0.77
Power per magnet weight	kW/kg	34.4	39.2	55.39	103.6	23.9	86.8	37.8	90.5	–	–
Power per current density	$kW/A/mm^2$	2.50	2.30	1.77	1.14	3.97	3.09	7.14	4.90	3.38	10.31

• Machines that are naturally cooled (HC) and less complexly cooled (HA) have poor torque and power densities. SPM topologies are also unsuitable for applications requiring a broad speed range due to their poor field weakening capacity.

• The BI machine is less complexly cooled because of its low current density. On the other hand, the machine's increased active material has allowed for the high power and torque. Additionally, to sum up the results of the compared. The torque density, power density, rotor peripheral speed, rotor mechanical stress, and necessary cooling techniques under standard and hairpin winding configurations are shown in research, Fig. 2. The mechanical stress is estimated at a speed of 15 krpm, whereas the peripheral speed is computed at the machine's base speed. The torque and power densities' current limits are 13 Nm/kg and 4.5 kW/kg, respectively, as shown in Fig. 2. Additionally, when more aggressive cooling techniques are used, torque and power density rise in tandem with time. In a similar vein, the torque and power densities correlate with increases in the rotor mechanical stress and peripheral speed throughout the timeline.

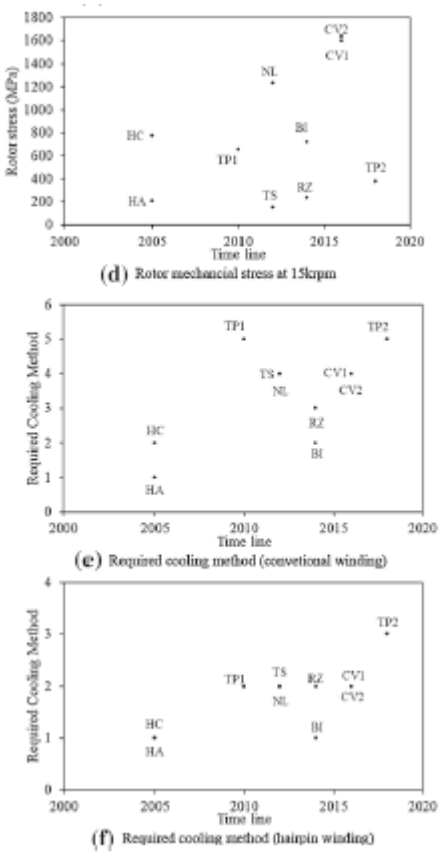

Figure 2: Electrical machine trend in both HEVs and EVs. Rotor peripheral speed at machine base speed (d) Motor density (a), power density (b), and torque density (c). Mechanical load on the rotor at 15 krpm (e) (f) Required cooling method (hairpin winding) Needed cooling method (conventional winding)

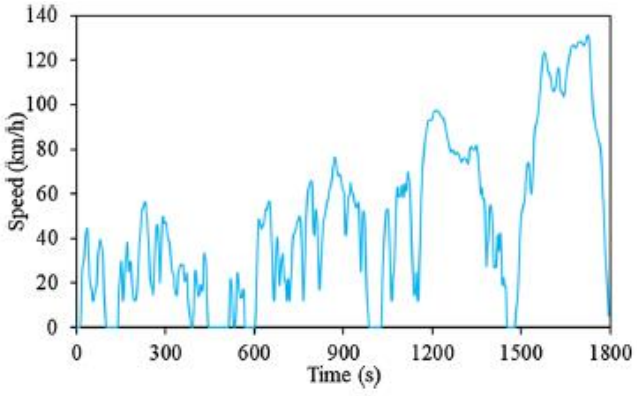

Fig. 3 WLTP driving cycle

Table 4 Electrical machine targets by the APC and FC [17, 18]

Performance	FC 2020	APC 2025	APC 2035
Continuous power density (kW/kg)	0.86	7	9
Continuous power per volume (kW/mm^3 E06)	1.82	25	30
300% material cost ($/kW)	33.25	5.8	4.5
WLTP drive cycle efficiency	82	92.5	93
DC voltage (V)	NS	350	350
Current (A)	NS	450	450
Cooling inlet temperature (C)	70	65	65

*NS not specified

4 Novel design standards for next automobile

The new European driving cycle (NEDC) will be replaced by the global harmonised light vehicle test procedure (WLTP) driving cycle by the end of 2019 for light-duty cars registered in the EU, Switzerland, Norway, Iceland, and Turkey. In Figure 3, the class 3 WLTP is shown. driving cycle [16]. As shown in Table 4 [17], the UK Advance Propulsion Centre (APC) has compiled the specifications for electric motors in automobiles to satisfy the legal requirements of 2025 and 2035. In a similar vein, Freedom-Car (FC), the counterpart in the USA, released the 2020 requirements [18]. Given a 100kW maximum output power, the torque-speed characteristic needed to satisfy the criteria has been estimated for various gearbox ratios and is shown in Figure 4. The goals for electrical machine design in the automobile industry to fulfil the performance requirement by 2035 are outlined below. On the other hand, cost requirements and material appropriateness are harder to measure; still, when designing electric machines for the automobile industry, low-cost, rare-earth steel grades and minimal copper usage should be taken into account.

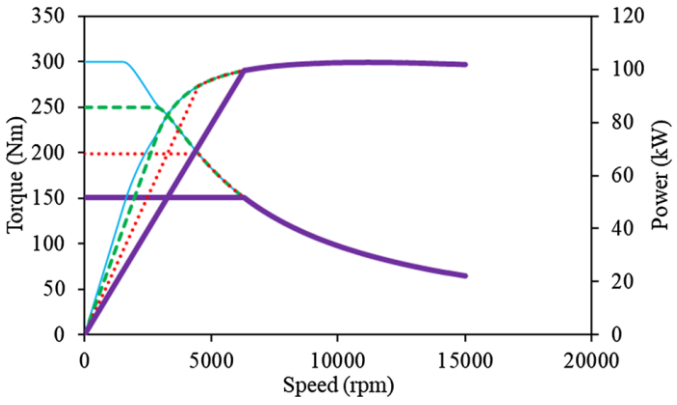

Fig. 4 Predicted torque-speed characteristics for future electrical machines in automotive

5 Designing techniques

5.1 Multi-objective optimization

Even though this hasn't been made a requirement for EVs, optimising electric vehicles aims to minimise energy use while simultaneously improving driving performance, lowering expenses, and remaining light in weight. It is essential that the problem be phrased to consider all of these conflicting aims simultaneously, since there isn't a single optimum solution that can meet them all. "Multi-objective optimisation" describes a technique that assists in identifying the best solutions that trade off a number of objectives. Multi-objective optimisation is yet another area of intense investigation. Finite element analysis (FEA) combined with optimisation algorithms like the genetic algorithm (GA), particle swarm optimisation (PSO) algorithm, non-dominated sorting genetic algorithm-II (NSGA-II), fuzzy method, and sequential Taguchi method is the most popular and extensively used technique for optimising electrical machines. Furthermore, a potential technique for effective multi-objective optimisation is the implementation of multilevel optimisation approach, particularly for optimisation techniques that must successfully address multi-parameter and multi-objective optimisation issues. The previously outlined techniques hold promise for the efficient multi-objective optimisation of electrical devices with large dimensions intended for use in the automobile sector.

Table 10 compares the AC loss at 5000 rpm of standard copper/aluminum windings (Cu/Al) versus hairpin copper/aluminum windings (CuH/Alh). The weight (kg), temperature (C), AC and DC loss (W)

		Kp	DC loss	AC loss	Total loss	Max Temp	Total weight	Max winding
HA	Cu	0.6	704.3	446	1150.3	150	106	22.86
	Cuh	0.77	501	3059	3560	217	75	24.98
	Al	0.6	1148	274	1422	168	135	19.07
	Alh	0.77	802	2369	3171	202	87	19.53
HC	Cu	0.6	888	478	1366	214	146	18.22
	Cuh	0.75	707	4029	4736	365	102	19.48
	Al	0.6	1448	293	1741	248	199	14.93
	Alh	0.75	1152	3157	4309	340	132	15.32
TP1	Cu	0.4	7952	246	8198	679	659	19.08
	Cuh	0.75	3123	2943	6066	313	162	23.53
	Al	0.4	12,960	151	13,111	1104	1107	16.51
	Alh	0.75	5347	2306	7653	379	286	17.26
TP2	Cu	0.4	11,130	930	12,060	905	865	15.33
	Cuh	0.72	5345	3560	8905	420	278	18.64
	Al	0.4	18,130	578	18,708	1455	1280	13.25
	Alh	0.72	8900	2331	11,231	525	421	13.82
CV1	Cu	0.4	3981	920	4901	350	243	30.15
	Cuh	0.7	2035	2640	4675	217	124	33.89
	Al	0.4	6487	673	7160	478	370	27.22
	Alh	0.7	3315	2068	5383	240	168	28.14
CV2	Cu	0.4	3442	541	3983	353	242	19.61
	Cuh	0.7	1760	1383	3143	187	124	22.53
	Al	0.4	5608	395	6003	495	367	16.79
	Alh	0.7	2866	1084	3950	220	177	17.55
BI	Cu	0.4	2405	2446	4851	90	75	46.51
	Cuh	0.63	1648	1859	3507	75	62	50.79
	Al	0.4	3918	1589	5507	117	103	41.12
	Alh	0.63	2692	1208	3900	92	76	43
NL	Cu	0.4	5059	696	5755	286	246	33.17
	Cuh	0.62	3670	983	4653	199	166	35.71
	Al	0.4	8244	427	8671	441	411	29.9
	Alh	0.62	5732	603	6335	269	246	31
RZ	Cu	0.4	4292	1083	5375	242	198	48.68
	Cuh	0.63	2787	1699	4486	195	131	51.93
	Al	0.4	7005	663	7668	354	330	44.49
	Alh	0.63	5029	1041	6070	241	270	46.09
TS	Cu	0.4	4390	344	4734	246	240	60.32
	Cuh	0.69	2782	1657	4439	133	112	65.09
	Al	0.4	7153	211	7364	465	441	55.68
	Alh	0.69	4328	1298	5626	174	157	57.4

6. Conclusion

In this article, cutting-edge automobile electrical machinery and design methodologies are compared. Ten designs with varying topologies and parameters that were based on the literature available on the market have been compared. In this comparison, the machines that use PM aided SynRel topologies have the greatest torque density and torque per volume together with the highest power density. By outlining the Advanced Propulsion Centre (APC) ambitions for 2035, projecting a torque-speed profile, and working towards the WLTP driving cycle, the future goals for electrical motors in automotive applications are shown. Moreover, cutting-edge design methodologies have been

examined by using them in diverse topologies to demonstrate the impact of these methods and their capacity to advance the designs towards future goals. Hairpin winding, complicated cooling, rotor mechanics, recyclable design, and reduced and rare-earth free machines are among the strategies under investigation. Higher heat dissipation and a notable decrease in the winding's loss density are two benefits of hairpin winding. Hairpin winding may thus be used to create a reduced temperature increase, smaller size, and greater power density. Semi-flooded complex cooling removes a lot of heat from the stator winding, increasing current density and, in turn, power density. On the other hand, problems with the air gap sleeve and sealing impair machine performance and increase assembly complexity. Ferrite, a rare-earth free machine, has potential applications in the automobile industry. Less weight is possible because to the low mass density; nevertheless, the ferrite's poor coercivity makes field weakening simpler. As a result, a field weakening more than 1 is often seen, which lowers the broad power capacity throughout the speed range. Lastly, aluminium hairpin winding offers the advantages of reduced AC loss, less weight, and cost-effectiveness combined with a promising design that can be recycled.

REFERENCES

1. Zeraoulia M, Benbouzid MEH, Diallo D (2006) Electric motor drive selection issues for HEV propulsion systems: a comparative study. IEEE Trans Veh Technol 55(6):1756–1764

2. Kimiabeigi M et al (2018) Production and application of HPMS recycled bonded permanent magnets for a traction motor application. IEEE Trans Ind Electron 65(5):3795–3804

3. Olszewski M (2006) Evaluation of the 2005 Honda Accord hybrid electric drive system. Oak ridge national laboratory, ORNL/TM2006/535.

4. Olszewski M (2011) Evaluation of the 2010 Toyota Prius hybrid synergy drive system. Oak ridge national laboratory, ORNL/TM-2010/253.

5. Zhu ZQ, ChuWQ, GuanY(2017) Quantitative comparison of electromagnetic performance of electrical machines for HEVs/EVs. CES Trans Electr Mach Syst 1(1):37–47

6. . Guan Y, Zhu ZQ, Afinowi IAA, Mipo JC Farah P (2014) Design of synchronous reluctance and permanent magnet synchronous reluctance machines for electric vehicle application. *2014 17th International Conference on Electrical Machines and Systems (ICEMS)*, Hangzhou, 2014, pp. 1853–1859.

7. Momen F, Rahman K, Son Y (2019) Electrical propulsion system design of chevrolet bolt battery electric vehicle. IEEE Trans Ind Appl 55(1):376–384

8. Jurkovic S, Rahman K, Bae B, Patel N and Savagian P, (2015) "Next generation chevy volt electric machines; design, optimization and control for performance and rare-earth mitigation," *2015 IEEE Energy Conversion Congress and Exposition (ECCE)*, Montreal, QC, 2015, pp. 5219-5226

9. Anwar, Mohammad, et al. (2015) Power Dense and Robust Traction Power Inverter for the Second-Generation Chevrolet Volt Extended-Range EV. *SAE Int J Altern Powertrains JSTOR*

10. Merwerth J (2014) The hybrid-synchronous machine of the new 642 BMW i3 and i8. BMW group. https://www.speakev.com/ 20140404_bmw-pdf

11. BMW (2017) Specifications. The new BMW i3. BMW Media Information. https://www.press.bmwgroup.com

12. Staton D and Goss J, (2017) Open Source Electric Motor Models for Commercial EV & Hybrid Traction Motors," 2017 CWIEME, Berlin, 2017.

13. Roggia S and. Iacchetti M, (2016) Open source electric motor models for commercial EV & hybrid traction motors. International conference on electrical machines ICEM, Lausanne,

14. Fedoseyev L, Pearce E (2016) Rotor assembly with heat pipe cooling system. U.S. Patent 2014036806A1

15. Kane M (2015) Renault electric motor production at Cleon. Renault Group.

16.WLTP Facts, What is WLTP. https://www.wltpfacts.eu/what-iswltp- how-will-it-work/

17. APC (2020) Electric Machines Roadmap. APC. https://www.apcuk.co.uk/app/uploads/2021/09/https___www.apcuk_.co_.uk_app_uploads_2021_02_Exec-summary-Technology-Roadmap-Electric-Machines-final.pdf

18. US Department of Energy (2011) Hybrid and Electric Propulsion.https://www1.eere.energy.gov/vehiclesandfuels/pdfs/mypp/3-2_hybr_elec_prop.pdf

19. Staton D (2018) Electric motor design: trade-off analysis.

CWIEME, Berlin

20. Afinowi IAA, Zhu ZQ, GuanY, Mipo JC and Farah P (2014) Performance analysis of switched-flux machines with hybrid NdFeB and ferrite magnets. *2014 17th International Conference on ElectricalMachines and Systems (ICEMS)*, Hangzhou, pp. 3110–3116.